Pairing correlations near a Kondo-destruction quantum critical point

J. H. Pixley, Lili Deng, Kevin Ingersent, and Qimiao Si

Phys. Rev. B **91**, 201109 — Published 26 May 2015

DOI: 10.1103/PhysRevB.91.201109

Pairing Correlations Near a Kondo-Destruction Quantum Critical Point

J. H. Pixley,[1,2] Lili Deng,[3] Kevin Ingersent,[3] and Qimiao Si[2]

[1]*Condensed Matter Theory Center and Joint Quantum Institute, Department of Physics, University of Maryland, College Park, Maryland 20742- 4111 USA*
[2]*Department of Physics and Astronomy, Rice University, Houston, Texas, 77005, USA*
[3]*Department of Physics, University of Florida, Gainesville, Florida 32611-8440, USA*

(Dated: January 30, 2015)

Motivated by the unconventional superconductivity observed in heavy-fermion metals, we investigate pairing susceptibilities near a continuous quantum phase transition of the Kondo-destruction type. We solve two-impurity Bose-Fermi Anderson models with Ising and Heisenberg forms of the interimpurity exchange interaction using continuous-time quantum Monte-Carlo and numerical renormalization-group methods. Each model exhibits a Kondo-destruction quantum critical point separating Kondo-screened and local-moment phases. For antiferromagnetic interimpurity exchange interactions, singlet pairing is found to be enhanced in the vicinity of the transition. Implications of this result for heavy-fermion superconductivity are discussed.

PACS numbers: 71.10.Hf, 71.27.+a, 75.20.Hr

A quantum critical point (QCP) arises when matter continuously transforms from one ground state to another [1]. Whether and how a magnetic QCP underlies unconventional superconductivity in correlated electron systems remains one of the central questions in condensed matter physics [2–4]. At a macroscopic level, a QCP is accompanied by an enhanced entropy [5]. At sufficiently low temperatures, in the proximity of a QCP, it is natural for the enhanced entropy to promote emergent phases such as superconductivity. At a microscopic level, however, how quantum criticality drives superconductivity remains an open issue. Developing an understanding of unconventional superconductivity is pertinent to a large list of correlated materials such as iron pnictides, copper oxides, organics, and heavy fermions.

An important opportunity for detailed exploration of this general issue is provided by heavy-fermion metals, in which many QCPs have been explicitly identified [3, 6]. Theoretical studies have shown that antiferromagnetic QCPs in a Kondo lattice system fall into two classes. Spin-density-wave (SDW) QCPs are described in the Landau framework of order-parameter fluctuations [7]. The other class of QCPs goes beyond the Landau approach by invoking a critical destruction of the Kondo effect [8, 9]. Distinctive features of this "local quantum criticality" include ω/T scaling in the spin susceptibility and the single-particle spectral function, vanishing of an additional energy scale, and a jump in the Fermi-surface volume. There is mounting experimental evidence for these characteristic properties, e.g., from inelastic neutron-scattering measurements on Au-doped $CeCu_6$ [10], scanning tunneling spectroscopy on $CeCoIn_5$ [11], Hall-effect and thermodynamic measurements on $YbRh_2Si_2$ [12], and magnetic quantum-oscillation measurements on $CeRhIn_5$ [13].

Given the considerable advances in the understanding of the unconventional quantum critical behavior of heavy fermions in the normal state, it is clearly important to address its implications for superconductivity. Theoretically, it remains an open question whether a Kondo-destruction QCP promotes unconventional superconductivity [14]. To make progress, it is essential to identify simplified models in which this issue can be addressed and insights can be gained. Because an on-site Coulomb repulsion does not favor conventional s-wave pairing, this issue can only be studied in models that incorporate correlations among different local-moment sites.

In this work, we propose perhaps the simplest models that support Kondo-destruction physics and allow the study of superconducting correlations: two local moments that interact with each other through a direct exchange interaction and are also coupled both to a conduction-electron band and to a bosonic bath. The models we have considered can be obtained from a cluster generalization of the extended dynamical mean field theory (C-EDMFT) [15] applied to the periodic Anderson model with Ising anisotropy. The critical physics arises from the antiferromagnetic channel, which we will be concerned with. We then arrive at the model defined in Eq. (1) below [15]. In the past, significant insights have been gained from single-impurity models, where Kondo-destruction QCPs are characterized by a vanishing Kondo energy scale, an ω/T scaling in the local spin susceptibility and a linear-in-temperature single-particle relaxation rate [16–21]. Such properties are reminiscent of the aforementioned experiments near the antiferromagnetic QCPs of heavy-fermion metals.

We solve the two-impurity Bose-Fermi Anderson models via a continuous-time quantum Monte-Carlo (CT-QMC) approach [19, 21, 22] and using the numerical renormalization group (NRG) [16, 23]. We determine the magnetic quantum critical properties and compute pairing susceptibilities across the phase diagram. We find that pairing correlations are in general enhanced

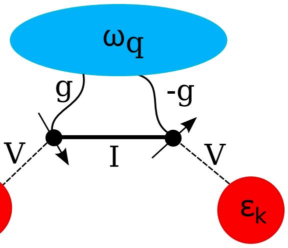

FIG. 1: (color online). Schematic representation of the two-impurity Bose-Fermi Anderson models considered in this work. The impurity spins interact via a direct exchange coupling I (or I_z), and $S_1^z - S_2^z$ couples with strength g to a dissipative bosonic bath having dispersion $\omega_{\mathbf{q}}$. For very large impurity separation, each impurity effectively hybridizes with strength V with its own conduction band of dispersion $\epsilon_{\mathbf{k}}$.

near the Kondo-destruction QCP. This suggests a new mechanism for superconductivity near antiferromagnetic quantum phase transitions (QPTs).

The two-impurity Bose-Fermi Anderson models, illustrated in Fig. 1, are defined by Hamiltonians of the form

$$H = \sum_{i=1,2}\left(\epsilon_d \sum_{\sigma} n_{di\sigma} + U n_{di\uparrow} n_{di\downarrow}\right) + H_{12} + \sum_{\mathbf{k},\sigma} \epsilon_{\mathbf{k}} c^{\dagger}_{\mathbf{k}\sigma} c_{\mathbf{k}\sigma} + \frac{V}{\sqrt{N_k}} \sum_{i,\mathbf{k},\sigma}\left(e^{i\mathbf{k}\cdot\mathbf{r}_i} d^{\dagger}_{i\sigma} c_{\mathbf{k}\sigma} + \text{H.c.}\right) + \sum_{\mathbf{q}} \omega_{\mathbf{q}} \phi^{\dagger}_{\mathbf{q}} \phi_{\mathbf{q}} + g(S_1^z - S_2^z)\sum_{\mathbf{q}}(\phi^{\dagger}_{\mathbf{q}} + \phi_{-\mathbf{q}}). \quad (1)$$

Here, $d_{i\sigma}$ destroys an electron on impurity site $i = 1$ or 2 with spin $\sigma = \uparrow$ or $\downarrow$, energy ϵ_d, and on-site Coulomb repulsion U; $n_{di\sigma} = d^{\dagger}_{i\sigma} d_{i\sigma}$, and $\mathbf{S}_i = \frac{1}{2}\sum_{\alpha,\beta} d^{\dagger}_{i\alpha} \boldsymbol{\sigma}_{\alpha\beta} d_{i\beta}$ where $\sigma^{x,y,z}_{\alpha\beta}$ are the Pauli matrices. The operator $c_{\mathbf{k}\sigma}$ destroys a conduction electron with wave vector $\mathbf{k}$, spin σ, and energy $\epsilon_{\mathbf{k}}$ that has a hybridization V with each impurity, while $\phi_{\mathbf{q}}$ destroys a boson with energy $\omega_{\mathbf{q}}$ that couples with strength g to the difference of impurity spin z components. N_k is the number of $\mathbf{k}$ values.

To control the interimpurity exchange interaction, we take the limit of infinite impurity separation $|\mathbf{r}_1 - \mathbf{r}_2|$ to ensure the vanishing of the indirect Ruderman-Kittel-Kasuya-Yosida exchange interaction between $\mathbf{S}_1$ and $\mathbf{S}_2$. Then impurities 1 and 2 hybridize with linearly independent combinations of band states, and interact only through their coupling to the bosonic bath and via a direct exchange term H_{12}, either of the Ising form $H_{12} = I_z S_1^z S_2^z$ or the Heisenberg form $H_{12} = I\mathbf{S}_1 \cdot \mathbf{S}_2$. Ising exchange is naturally obtained from the C-EDMFT approach [15], but including the static Heisenberg interaction allows us to study anisotropic couplings since this breaks the purely Ising coupling of the bosonic bath. We note that integrating out the bosonic bath will induce a retarded antiferromagnetic exchange of Ising symmetry.

We assume a flat electronic density of states $\rho_c(\epsilon) = \rho_0 \Theta(D - |\epsilon|)$ and a sub-Ohmic bosonic density of states

$$\rho_\phi(\omega) = K_0^2 \omega_c^{1-s} \omega^s \,\Theta(\omega)\, f(\omega/\omega_c). \quad (2)$$

For the CT-QMC calculations we have used a cutoff function $f(x) = \exp(-|x|)$ and chosen $K_0^{-2} = \omega_c^2 \Gamma(s+1)$ so that the density of states is normalized to unity. Within the NRG, we use $f(x) = \Theta(1 - |x|)$ with $K_0 = 1$. In this work we restrict ourselves to the range $1/2 < s < 1$.

In the absence of the bosonic bath, the pure-fermionic two-impurity Anderson model can be mapped via a Schrieffer-Wolff transformation to a two-impurity Kondo model with a direct exchange interaction [24]. In the case of Heisenberg exchange, both the Anderson and Kondo formulations are well studied [25, 26], displaying a critical point at an antiferromagnetic exchange $I_c > 0$ in the presence of particle-hole symmetry; at this point, the static singlet-pairing susceptibility diverges [27]. For an Ising H_{12}, the model possesses a Kosterlitz-Thouless (KT) QPT at $|I_z^c| > 0$ between a Kondo-screened phase and an interimpurity Ising-ordered phase [28, 29]. Without the conduction band, Eq. (1) reduces to a two-spin boson model; studies of this model with $S_1^z + S_2^z$ coupled to a spin bath found a QCP separating a delocalized phase and a ferromagnetically localized phase [30, 31].

We have solved Eq. (1) with H_{12} of Ising form by extending the CT-QMC approach [19, 21, 22]. We determine the staggered Binder cumulant [20, 21, 32] $U_4^s(\beta, I_z, g) = \langle M_s^4\rangle / \langle M_s^2\rangle^2$, where the staggered magnetization $M_s = \beta^{-1}\int_0^\beta d\tau\, S_s^z(\tau)$ with $S_s^z = \frac{1}{2}(S_1^z - S_2^z)$, and the staggered static spin susceptibility $\chi_s(T) = \beta\langle M_s^2\rangle$. The Heisenberg form of H_{12} we have solved using the Bose-Fermi extension [16] of the NRG [23, 33]. To measure the pairing correlation between the d-electrons at different impurity sites, we study dynamic singlet (d-wave) and triplet (p-wave) pairing susceptibilities

$$\chi_\alpha(\tau, \beta) = \langle T_\tau \Delta_\alpha(\tau) \Delta^{\dagger}_\alpha\rangle, \quad \alpha = d \text{ or } p, \quad (3)$$

where $\Delta^{\dagger}_d = \frac{1}{\sqrt{2}}(d^{\dagger}_{1\uparrow} d^{\dagger}_{2\downarrow} - d^{\dagger}_{1\downarrow} d^{\dagger}_{2\uparrow})$, $\Delta^{\dagger}_p = \frac{1}{\sqrt{2}}(d^{\dagger}_{1\uparrow} d^{\dagger}_{2\uparrow} + d^{\dagger}_{1\downarrow} d^{\dagger}_{2\downarrow})$, and T_τ orders in imaginary time. The static pairing susceptibilities follow via $\chi_\alpha(T) = \int_0^\beta d\tau\, \chi_\alpha(\tau, \beta)$. Each numerical technique as applied to the models studied here is further described in the supplementary material [34], and additional details will be given elsewhere [35].

In the following, we work with fixed $\Gamma_0 = 0.25D$ and $U = -2\epsilon_d = 0.001D$. This choice places the Anderson impurities at mixed valence with a high Kondo temperature $T_K \simeq 1.39D$ (for $g, I_z, I = 0$), ensuring a correspondingly high temperature of entry into the quantum critical regime [21]. We also take $\omega_c = D$ and focus on sub-Ohmic bath exponents [see Eq. (2)] $s = 0.8$ for Ising exchange and $s = 0.6$ for the Heisenberg case.

Ising H_{12}: Figure 2(a) shows the $T = 0$ phase diagram for the case of Ising exchange, as obtained using CT-QMC. For $0 \le g, I_z \ll D$, each impurity spin is

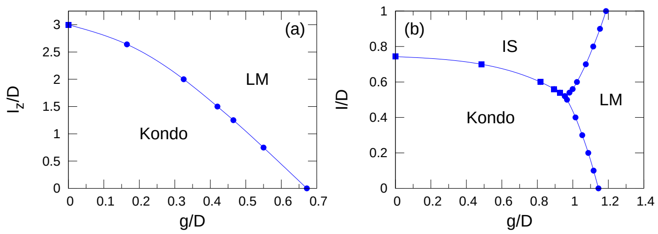

FIG. 2: (color online). (a) Phase diagram for an Ising H_{12} determined via CT-QMC from the staggered Binder cumulant. A square marks the Kosterlitz-Thouless QPT and circles denote second-order Kondo-destruction QPTs governed by the QCP at $I_z = 0$. (b) Phase diagram for a Heisenberg H_{12} found with the NRG. Squares represent QPTs governed by the critical point at $g = 0$, while circles represent Kondo-destruction QPTs induced by the coupling to the bosonic bath. Kondo-screened (Kondo), interimpurity-singlet (IS), and local-moment (LM) phases all meet at a tricritical point.

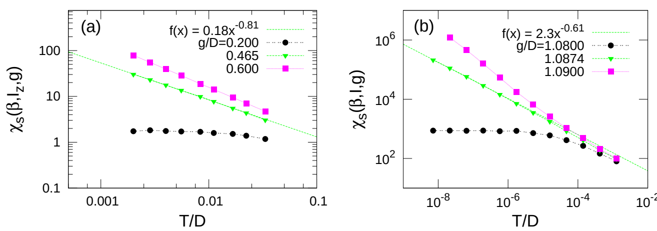

FIG. 3: (color online). Staggered spin susceptibility $\chi_s(T)$ in the Kondo phase (circles), at the QCP (triangles), and in the LM phase (squares), for (a) an Ising H_{12} with $s = 0.8$, and (b) a Heisenberg H_{12} with $s = 0.6$. At the QCP, $\chi_s \sim T^{-s}$.

locked into a Kondo singlet with the conduction band and $\chi_s(T)$ approaches a constant at low temperatures [e.g., Fig. 3(a)]. Upon increasing g and/or I_z, the system passes through a QPT into an Ising-antiferromagnetic local-moment phase (LM) in which the impurity spins are anti-aligned and decoupled from the conduction band, as seen through a Curie-Weiss behavior of the staggered spin susceptibility: $\chi_s(T) \sim T^{-1}$ [Fig. 3(a)]. The Kondo energy scale vanishes continuously on the Kondo side of the QPT, characteristic of a Kondo-destruction QCP. The staggered Binder cumulant $U_4^s(\beta, I_z, g)$ varies from 3 deep in the Kondo phase to 1 far into the LM phase. For fixed I_z, the cumulant near the QCP has a scaling form

$$U_4^s(\beta, I_z, g) = U_4^s\big(\beta^{1/\nu}(g/g_c - 1); I_z\big), \qquad (4)$$

identifying g_c as the point of temperature independence of U_4^s vs g [Fig. 4(a)]. Optimizing the scaling collapse according to Eq. (4) gives a correlation-length exponent $\nu(s = 0.8)^{-1} = 0.45(8)$ [Fig. 4(b)], close to the value 0.469(1) found using the NRG for the single-impurity Ising-symmetry Bose-Fermi Kondo model [16].

For $g = 0$, the Ising critical point is KT-like, characterized by a divergence $\chi_s(T, I_z = I_z^c, g = 0) \sim T^{-1}$. Consequently, the coupling g has a scaling dimension

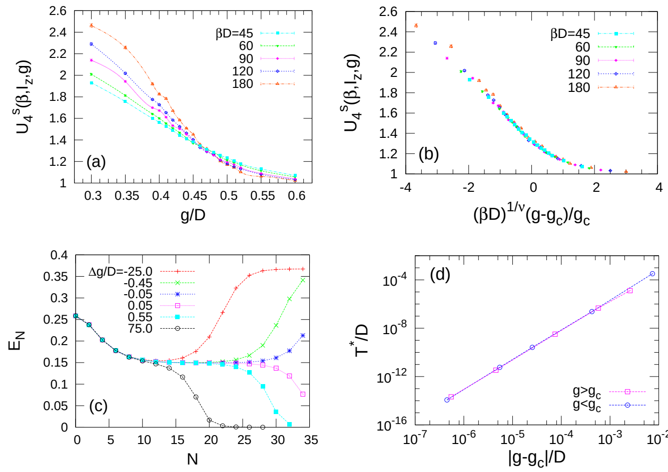

FIG. 4: (color online). (a) Binder cumulant $U_4^s(\beta, I_z, g)$ vs g for an Ising H_{12} with $I_z = 1.25D$, $s = 0.8$, and at the labeled temperatures. The intersection of curves gives the critical bosonic coupling $g_c/D = 0.465(5)$. (b) A scaling collapse of the same data near g_c according to Eq. (4) yields a correlation-length exponent $\nu(s = 0.8)^{-1} = 0.45(8)$. (c) Flow of a low-energy NRG eigenstate vs iteration number N for a Heisenberg H_{12} with $I = 0.2D$, $s = 0.6$, and six values of $\Delta g \equiv 10^6(g - g_c)$, where $K_0 g_c = 1.08742545(1)$. (d) Low-energy crossover scale from the NRG, fitted to $T^* \propto |g - g_c|^\nu$ yielding $\nu(s = 0.6)^{-1} = 0.40(2)$.

$[g] = (1 - s)/2$ and is relevant for $s < 1$. This dictates a flow away from the KT fixed point along the phase boundary in Fig. 2(a) toward the $I_z = 0$ critical point [34]. Tuning g to the boundary at fixed $I_z > 0$, we find that the staggered spin susceptibility diverges as

$$\chi_s\big(T, I_z, g = g_c(I_z)\big) \sim T^{-x} \qquad (5)$$

with $x = 0.79(3), 0.78(3), 0.80(3), 0.82(3), 0.82(3), 0.83(4)$ for increasing I_z. These values are consistent with $x = s$, suggesting that the staggered channel exhibits the same critical properties as the single-impurity Ising-symmetric Bose-Fermi Kondo model [16].

Heisenberg H_{12}: For Heisenberg exchange, the NRG gives the phase diagram shown in Fig. 2(b), based on runs performed with a basis of up to $N_b = 4$ bosons per site of the bosonic Wilson chain and retaining up to $N_s = 800$ many-body eigenstates at the end of each iteration. For small g and I, the model is in the Kondo phase. Tuning I for $g = 0$, we pass through a critical point into an interimpurity singlet (IS) phase, in which the impurity spins are locked into a singlet and decoupled from the conduction band. At the particle-hole-symmetric critical point [25, 26], the staggered spin susceptibility diverges as $\chi_s(T, I = I_c, g = 0) \sim \ln(T_K/T)$. Using the corresponding scaling dimension of the staggered impurity spin, along with the scaling dimension of $\phi_{\mathbf{q}}$, we determine that the bosonic coupling has scaling dimension $[g] = -s/2$ and is irrelevant for $s > 0$. Indeed, we find that the NRG spectrum along the phase boundary is independent of g for small values of g [34], indicating that the critical behavior is governed by the $g = 0$ QCP.

For small $I > 0$, tuning the bosonic coupling g yields a QPT from the Kondo phase to the LM phase [Fig. 4(c)]. The Kondo energy scale vanishes continuously on approach from the small-g side of this Kondo-destruction QCP. At the QCP, the staggered spin susceptibility obeys Eq. (5) with I_z replaced by I and $x = 0.61(2)$ [Fig. 3(b)], again consistent with $x = s$. Nearby, a low-energy crossover temperature T^* (equal to the effective Kondo temperature for $g < g_c$) varies as $T^* \propto |g - g_c|^{\nu}$, yielding for the data shown in Fig. 4(d) a correlation-length exponent $\nu(s = 0.6)^{-1} = 0.40(2)$. However, we find that (unlike the global phase diagram and the value of the exponent x), the value of ν is sensitive to the NRG truncation of states. Increasing N_b from 4 to 6 and N_s from 800 to 1 200 leads to a refinement of our estimate to $\nu(s = 0.6)^{-1} = 0.51(4)$, within numerical error identical to the value $\nu(s = 0.6)^{-1} = 0.509(1)$ found for the single-impurity Ising-symmetry Bose-Fermi Kondo model [16]. We therefore conclude that the Kondo-destruction QCPs for Ising and Heisenberg exchange fall within the same universality class. In both Ising and Heisenberg cases, the Kondo-destruction QCPs are insensitive to breaking of particle-hole symmetry via setting $U \neq -2\epsilon_d$, as well as to a finite impurity separation [35].

We turn next to the transition between the IS and LM phases. Fixing I at a large value and tuning g, the bosonic bath decoheres and destroys the interimpurity singlet state at a QCP, where we find similar critical properties to those on the Kondo-LM boundary: χ_s diverging according to Eq. (5) with $x = 0.61(3)$, and for $N_b = 4$, a correlation length exponent $\nu(s = 0.6)^{-1} = 0.40(2)$ indistinguishable from the corresponding value found on the Kondo-LM boundary.

In the particle-hole symmetric case that is the focus of this paper, the Kondo, IS, and LM phases all meet at a tricritical point, as shown in Fig. 2(b). Generic particle-hole asymmetry is known to turn the Kondo-to-IS transition in figure 2(b) into a crossover [25, 26], leaving only a single line of Kondo-destruction QPTs.

Pairing susceptibilities: We now consider the singlet and triplet pairing susceptibilities defined in Eq. (3). For both the Ising and Heisenberg forms of the interimpurity exchange, the static triplet pairing susceptibility χ_p (not shown) is reduced by any nonzero value of g, I_z, or I.

More interesting is the singlet susceptibility, which we illustrate along paths on the g-I_z and g-I phase diagrams that start from $g = I_z = I = 0$ and cross the Kondo-LM boundary. In C-EDMFT [15] such trajectories are representative of tuning spin-spin interactions within the lattice model. Figure 5(a) plots χ_d vs Ising exchange coupling at a sequence of temperatures along the cut $g = 0.372I_z$. The pairing susceptibility grows as I_z increases from zero, is peaked for I_z slightly below I_z^c, and then falls

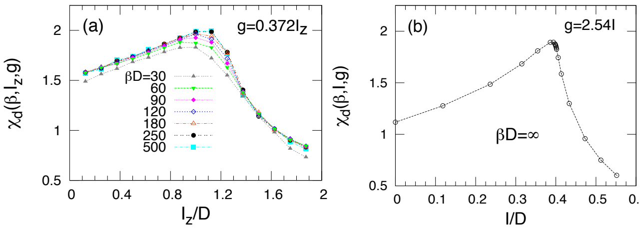

FIG. 5: (color online). (a) Static singlet pairing susceptibility $\chi_d(T, I_z, g)$ vs I_z for an Ising H_{12} with $s = 0.8$ along the line $g = 0.372I_z$, which crosses the Kondo-LM phase boundary at $I_z^c = 1.25D$. (b) Static singlet pairing susceptibility $\chi_d(T = 0, I, g)$ vs I for a Heisenberg H_{12} with $s = 0.6$ along the line $g = 2.54I$, which crosses the Kondo-LM phase boundary at $I_c = 0.40D$. In both (a) and (b), χ_d is peaked just on the Kondo side of the phase boundary and remains elevated at the QCP over its value for $g = I_z = I = 0$.

off within the LM phase as the d electrons localize and decouple from the conduction band. The singlet pairing susceptibility saturates at temperatures $T \lesssim 0.003T_K$.

Figure 5(b) illustrates the Heisenberg form of H_{12}, plotting the $T = 0$ singlet pairing susceptibility vs I at $T = 0$ along a path $g = 2.54I$ that crosses the Kondo-LM boundary. Very much as in the Ising case, χ_d rises from $I = 0$ and peaks just below $I = I_c$.

The enhancement of the static singlet pairing susceptibility near a Kondo-destruction QCP is one of the principal results of this work. Although χ_d peaks just inside the Kondo phase, the pairing correlation at the QCP is significantly higher than at $g = I_z = I = 0$. We stress that these results are associated with the critical destruction of the Kondo effect. They differ from those for $g = 0$, where for Heisenberg exchange $\chi_d(T = 0)$ diverges at the Kondo-IS QPT [27]. We have found (by following the path $g = 0.717I$, not shown) that the singlet pairing susceptibility also diverges on crossing the Kondo-IS boundary at some $g > 0$, consistent with the picture that this boundary is governed by the $g = 0$ critical point.

The models considered here have both a dynamic (induced by g) and a static (I_z or I) exchange interaction between the impurities. The combination of the two antiferromagnetic interactions is responsible for both, the existence of a Kondo-destruction QCP and the enhancement of χ_d in its vicinity. This behavior is likely to have significant effects in lattice systems. Within C-EDMFT [15], the cluster pairing susceptibility determines the lattice pairing susceptibility, in such a way that the enhanced χ_d may give rise to a pairing instability near a Fermi-surface-collapsing QCP of a Kondo lattice [8, 9]. As such, this would represent a new mechanism for superconductivity in the vicinity of antiferromagnetic order, and would be of considerable interest in connection with the superconductivity observed in the Ce-115 materials [37] and related heavy-fermion superconductors [38].

In summary, we have introduced and solved two variants of the two-impurity Bose-Fermi Anderson model using robust numerical methods. We have mapped out the phase diagrams for these models and shown that each possesses a line of Kondo-destruction QCPs that are insensitive to breaking particle-hole symmetry. The QCPs in the two models belong to the same universality class despite the differing symmetries of the interimpurity exchange interaction. Just as importantly, we have shown that the Kondo-destruction quantum criticality in these models *enhances* singlet pairing correlations. Our results hold promise for elucidating the superconductivity observed in heavy-fermion metals whose normal state shows characteristics of Kondo-destruction quantum criticality.

We acknowledge useful discussions with Stefan Kirchner, Lijun Zhu, Aditya Shashi, and Ang Cai. This work was supported in part by NSF Grants No. DMR-1309531 and No. DMR-1107814, Robert A. Welch Foundation Grant No. C-1411, the East-DeMarco fellowship (JHP), and the Alexander von Humboldt Foundation. Computer time and IT support at Rice University was supported in part by the Data Analysis and Visualization Cyberinfrastructure funded by NSF under Grant No. OCI-0959097. J.H.P. acknowledges the hospitality of the Max Planck Institute for the Physics of Complex Systems, and Q.S. acknowledges the hospitality of the the Karlsruhe Institute of Technology, the Aspen Center for Physics (NSF Grant No. 1066293), and the Institute of Physics of Chinese Academy of Sciences.

[1] Special issue: Quantum Phase Transitions. J. Low Temp. Phys. **161**, 1-323 (2010).
[2] P. Coleman and A. J. Schofield, Nature **433**, 226 (2005).
[3] Q. Si and F. Steglich, Science **329**, 1161 (2010)
[4] N.D. Mathur, F.M. Grosche, S.R. Julian, I.R. Walker, D.M. Freye, R.K.W. Haselwimmer and G.G. Lonzarich, Nature **394**, 39-43 (1998).
[5] J. Wu, L. Zhu and Q. Si, J. Phys.: Conf. Ser. **273**, 012019 (2011).
[6] H. v. Löhneysen, A. Rosch, M. Vojta and P. Wölfe, Rev. Mod. Phys., **79**, 1015 (2007)
[7] J. A. Hertz, Phys. Rev. B **14**, 1165, (1976); A. J. Millis, *ibid.* **48**, 7183, (1993).
[8] Q. Si, S. Rabello, K. Ingersent and J. L. Smith, Nature **413**, 804 (2001); Phys. Rev. B **68**, 115103 (2003).
[9] P. Coleman, C. Pépin, Q. Si and R. Ramazashvili, J. Phys. Cond. Matt. **13**, R723 (2001).
[10] A. Schröder, G. Aeppli, R. Coldea, M. Adams, O. Stockert, H. v. Löhneysen, E. Bucher R. Ramazashvili and P. Coleman, 2000 Nature **407**, 351 (2000); M. C. Aronson, R. Osborn, R. A. Robinson, J. W. Lynn, R. Chau, C. L. Seaman and M. B. Maple, Phys. Rev. Lett. **75**, 725 (1995).
[11] P. Aynajian, E. H. da Silva Neto, A. Gyenis, R. E. Baumbach, J. D. Thompson, Z. Fisk, E. D. Bauer, and A. Yazdani, Nature **486**, 201 (2012).
[12] S. Paschen, T. Lühmann, S. Wirth, P. Gegenwart, O. Trovarelli, C. Geibel, F. Steglich, P. Coleman and Q. Si, Nature **432**, 881 (2004); P. Gegenwart, T. Westerkamp, C. Krellner, Y. Tokiwa, S. Paschen, C. Geibel, F. Steglich, E. Abrahams, Q. Si, Science, **315**, 969 (2007); S. Friedemann, N. Oeschler, S. Wirth, C. Krellner, C. Geibel, F. Steglich, S. Paschen, S. Kirchner and Q. Si, Proc. Natl. Acad. Sci. USA **107**, 14547 (2010).
[13] H. Shishido, R. Settai, H. Harima, and Y. Ōnuki, J. Phys. Soc. Jpn. **74**, 1103 (2005).
[14] P. Gegenwart, Q. Si and F. Steglich, Nat. Phys. **4**, 186 (2008).
[15] J. H. Pixley, A. Cai, and Q. Si, arXiv:1409.1090 (2014).
[16] M. T. Glossop and K. Ingersent Phys. Rev. Lett. **95**, 067202 (2005); Phys. Rev. B **75**, 104410 (2007).
[17] K. Ingersent and Q. Si Phys. Rev. Lett. **89**, 076403 (2002).
[18] S. Kirchner and Q. Si Phys. Rev. Lett. **100**, 026403 (2008).
[19] J. H. Pixley S. Kirchner M. T. Glossop and Q. Si, J. Phys.: Conf. Ser. **273**, 012050 (2011).
[20] M. T. Glossop, S. Kirchner, J. H. Pixley, and Q. Si, Phys. Rev. Lett. **107**, 076404 (2011); J. H. Pixley, S. Kirchner, K. Ingersent, and Q. Si, *ibid.* **109**, 086403 (2012).
[21] J. H. Pixley, S. Kirchner, K. Ingersent, and Q. Si, Phys. Rev. B **88**, 245111 (2013).
[22] E. Gull, A. J. Millis, A. I. Lichtenstein, A. N. Rubtsov, M. Troyer, and P. Werner, Rev. Mod. Phys. **83**, 349 (2011).
[23] K. G. Wilson, Rev. Mod. Phys. **47**, 773 (1975).
[24] L. J. Zhou and Q. Q. Zheng, J. Magn. & Magn. Mater. **109**, 237 (1992); T. T. Ong and B. A. Jones, Euro. Phys. Lett. **93**, 57004 (2011).
[25] B. A. Jones and C. M. Varma, Phys. Rev. Lett. **58**, 843 (1987); B. A. Jones, C. M. Varma and J. W. Wilkins, *ibid.* **61**, 125 (1988); B. A. Jones, B. G. Kotliar and A. J. Millis, Phys. Rev. B **39**, 3415 (1989); R. M. Fye, Phys. Rev. Lett. **72**, 916 (1994); L. Zhu and J. X. Zhu, Phys. Rev. B **83**, 195103 (2011); L. Zhu and J. X. Zhu, *ibid.* **87**, 085120 (2013).
[26] I. Affleck and A. W. W. Ludwig, Phys. Rev. Lett. **68**, 1046 (1992); I. Affleck, A. W. W. Ludwig and B. A. Jones Phys. Rev. B **52**, 9528 (1995).
[27] L. Zhu and J. X. Zhu, J. Phys.: Conf. Ser. **273**, 012068 (2011).
[28] N. Andrei, G. T. Zimanyi, and G. Schön, Phys. Rev. B **60**, R5125 (1999).
[29] M. Garst, S. Kehrein, T. Pruschke, A. Rosch, and M. Vojta, Phys. Rev. B **69**, 214413 (2004).
[30] P. P. Orth, D. Roosen, W. Hofstetter, and K. Le Hur, Phys. Rev. B **82**, 144423 (2010).
[31] D. P. S. McCutcheon, A. Nazir, S. Bose, and A. J. Fisher, Phys. Rev. B **81**, 235321 (2010).
[32] K. Binder Z. Phys. B **43**, 119 (1981).
[33] R. Bulla, T. A. Costi, and Th. Pruschke, Rev. Mod. Phys. **80**, 395 (2008).
[34] See supplementary information at http://
[35] J. H. Pixley, L. Deng, K. Ingersent and Q. Si, in preparation
[36] J. L. Smith and Q. Si, Phys. Rev. B **61**, 5184 (2000); R. Chitra and G. Kotliar, Phys. Rev. Lett. **84**, 3678 (2000).
[37] H. Hegger, C. Petrovic, E. G. Moshopoulou, M. F. Hundley, J. L. Sarrao, Z. Fisk, and J. D. Thompson, Phys. Rev. Lett. **84**, 4986 (2000).

[38] Q. Si and S. Paschen, Phys. Status Solidi B **250**, 425 (2013).